Acta Cryst. (1990). A**46**, 821-826

Wavelength Dependence of the Reflectivity in Neutron Diffraction by Perfect Vibrating Crystals

BY J. P. GUIGAY

Laboratoire Louis Néel, CNRS, 166X, 38042 Grenoble CEDEX, France

P. MIKULA

Nuclear Physics Institute, Czechoslovak Academy of Sciences, CS-250 68 Rez near Prague, Czechoslovakia

R. HOCK

ILL, Grenoble, France

J. BARUCHEL

Laboratoire Louis Néel, CNRS, 166X, 38042 Grenoble CEDEX, France and ILL, Grenoble, France

AND A. WAINTAL

Laboratoire Louis Néel, CNRS, 166X, 38042 Grenoble CEDEX, France

(*Received* 28 *September* 1989; *accepted* 9 *May* 1990)

Abstract

The neutron reflectivity of low-frequency vibrating nearly perfect crystals has been measured as a function of the neutron wavelength, the displacement field being parallel to the diffraction vector. In Bragg symmetrical geometry, the experimental results can be explained using a dynamical theory of diffraction by one-dimensionally distorted crystals [Guigay (1986). *Acta Cryst.* A**42**, 481-483]. In Laue symmetrical geometry, it is shown that it is necessary to distinguish the cases of very small and less-small amplitudes of vibration.

1. Introduction

The aim of the present paper is to investigate the wavelength dependence of the reflectivity in symmetrical diffraction geometries (Bragg or Laue), for crystals displaying a one-dimensional deformation along the scattering vector. These conditions can be approximated by a perfect vibrating crystal such that the frequency of the vibrations is low enough to consider the displacement of atoms seen by the incident neutrons as a static one. In this paper absorption effects are assumed to be negligible.

For Bragg symmetrical geometry, when the Bragg angle θ_B is varied by changing the neutron wavelength λ, the integrated reflectivities ρ_D and ρ_K of perfect and ideally imperfect crystals are both proportional to $\tan\theta_B$. This property can be shown from the well known formulas:

$$\rho_K = Ql = Ql_0/\sin\theta_B \qquad (1)$$

$$\rho_D = Q\Lambda \tanh(l/\Lambda). \qquad (2)$$

Here, l is the path length in the crystal along the incident direction, l_0 is the crystal thickness and Λ is the extinction length defined as

$$\Lambda = V_c/\lambda F \qquad (3)$$

where V_c is the volume of the unit cell and F is the structure factor of the considered reflection. The ratio l/Λ does not depend on θ_B since $\lambda/2\sin\theta_B$ is the spacing of the reflecting planes. Q is, as usual, the kinematical reflectivity per unit path length:

$$Q = \frac{\lambda}{\Lambda^2 \sin 2\theta_B} = \frac{\lambda^3 F^2}{V_c^2 \sin 2\theta_B}. \qquad (4)$$

It is easily seen from (1) and (4) that

$$\rho_K = \frac{l_0 F^2}{2V_c^2}\left(\frac{\lambda}{\sin\theta_B}\right)^3 \tan\theta_B \qquad (5)$$

is indeed proportional to $\tan\theta_B$. $Q\Lambda$ is also found to be proportional to $\tan\theta_B$ and, consequently (since l/Λ does not depend on θ_B), ρ_D also follows this dependence. Under what conditions should the reflectivity of a neither perfect nor ideally imperfect crystal also be proportional to $\tan\theta_B$? As shown earlier from Takagi-Taupin equations (Guigay, 1986), this is realized if the component of the displacement field in the direction of the diffraction vector $\mathbf{h}$ is uniform in any plane parallel to the surface.

In symmetrical Laue geometry, the kinematical reflectivity is proportional to $(\tan\theta_B)^2$ since $l = l_0/\cos\theta_B$ in this case, but the proportionality to $\tan\theta_B$ is still valid for a thick perfect crystal. Our purpose was then to test the ranges of validity of these $\tan\theta_B$ and $(\tan\theta_B)^2$ dependences. The experiments

0108-7673/90/100821-06$03.00

described in § 3.2 show that the $(\tan\theta_B)^2$ dependence is satisfied even when the reflectivity is still far from the kinematical value which might be obtained only with very large vibration amplitudes. The limiting case of the transition from the reflectivity of a slightly deformed crystal to the reflectivity of a perfect one for Laüe diffraction geometry have been recently described theoretically by Kulda & Lukáš (1989).

Approximate treatments of neutron diffraction by vibrating crystals have been given by Michalec, Chalupa, Sedláková, Mikula, Petržilka & Zelenka (1974) and by Michalec, Mikula, Vrána, Kulda, Chalupa & Sedláková (1988). A more general treatment has been given by Kulda, Vrána & Mikula (1988).

2. The symmetrical Bragg case

2.1. *Theoretical background*

Let us recall the Takagi–Taupin equations (Takagi, 1962, 1969; Taupin, 1964), using the oblique coordinate system (s_0, s_h) defined by the directions of the incident and diffracted plane waves corresponding to the exact Bragg orientation:

$$\begin{aligned}\Lambda\frac{\partial D_0}{\partial s_0} &= i\exp\{i\mathbf{h}\,.\,\mathbf{u}(s_0, s_h)\}D_h(s_0, s_h)\\ \Lambda\frac{\partial D_h}{\partial s_h} &= i\exp\{-i\mathbf{h}\,.\,\mathbf{u}(s_0, s_h)\}D_0(s_0, s_h)\end{aligned}\tag{6}$$

where $\mathbf{u}(s_0, s_h)$ is the displacement field describing the crystal deformation and $\mathbf{h}$ the diffraction vector.

Following the theoretical treatment of Guigay (1986), it is convenient to use the rectangular coordinates (x, z) such that (Fig. 1)

$$\begin{aligned}x &= (s_0+s_h)\cos\theta_B\\ z &= (s_0-s_h)\sin\theta_B.\end{aligned}\tag{7}$$

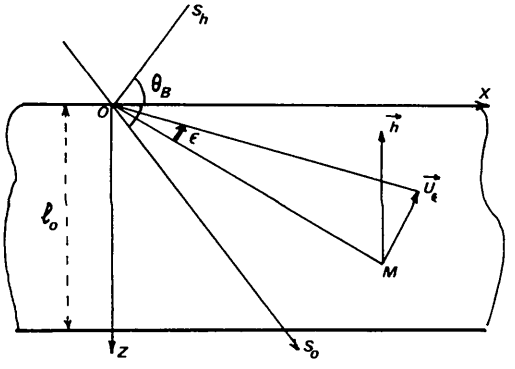

Fig. 1. Illustration of the displacement field $\mathbf{u}_\varepsilon(x, z)$ corresponding to a rotation of the crystal around the origin of coordinates in the symmetrical Bragg case. Since ε is small, the angles $(\mathbf{u}_\varepsilon, \mathbf{h})$ and (OM, Ox) are equal. So $\mathbf{h}\,.\,\mathbf{u}_\varepsilon = h\varepsilon x$. The position of point O is, of course, arbitrary; this is verified from the facts that $\mathbf{h}\,.\,\mathbf{u}_\varepsilon$ does not depend on z and that only the derivative $h\varepsilon$ of $h\varepsilon x$ is present in (11).

We shall consider a one-dimensional deformation such that the phase factor $\exp(i\mathbf{h}\,.\,\mathbf{u})$ is a function $\varphi(z)$ of the single variable z (no dependence on x).

The integrated reflectivity is obtained by considering the crystal rotating around its Bragg position for a fixed incident plane wave. This rotation defined by $\varepsilon = \theta - \theta_B$ can be viewed as a displacement field $\mathbf{u}_\varepsilon(x, z)$. From simple geometrical arguments illustrated in Fig. 1, it can be seen that

$$\mathbf{h}\,.\,\mathbf{u}_\varepsilon(x, z) = h\varepsilon x \tag{8}$$

which must be added to $\varphi(z)$; our basic equations are then

$$\begin{aligned}&\Lambda\cos\theta_B\,\partial D_0/\partial x + \Lambda\sin\theta_B\,\partial D_0/\partial z\\ &\quad= \exp\{i\varphi(z) + ih\varepsilon x\}D_h(\varepsilon, x, z)\\ &\Lambda\cos\theta_B\,\partial D_h/\partial x - \Lambda\sin\theta_B\,\partial D_h/\partial z\\ &\quad= \exp\{-i\varphi(z) - ih\varepsilon x\}D_0(\varepsilon, x, z).\end{aligned}\tag{9}$$

With the boundary conditions (l_0 being the crystal thickness)

$$\begin{aligned}D_0(\varepsilon, x, 0) &= 1\\ D_h(\varepsilon, x, l_0) &= 0,\end{aligned}\tag{9'}$$

we have indicated in (9) and (9') the ε dependence of the wave amplitudes $D_0(\varepsilon, x, z)$ and $D_h(\varepsilon, x, z)$.

Let us introduce the transformation

$$\begin{aligned}X_0(\varepsilon, x, z) &= D_0(\varepsilon, x, z)\\ X_h(\varepsilon, x, z) &= D_h(\varepsilon, x, z)\exp\{i\varepsilon hx\}.\end{aligned}\tag{10}$$

We get

$$\begin{aligned}&\Lambda\cos\theta_B\partial X_0/\partial x + \Lambda\sin\theta_B\partial X_0/\partial z\\ &\quad= i\exp\{i\varphi(z)\}X_h(x, z)\\ &\Lambda\cos\theta_B\{\partial X_h/\partial x - ih\varepsilon X_h\} - \Lambda\sin\theta_B\,\partial X_h/\partial z\\ &\quad= i\exp\{-i\varphi(z)\}X_0(x, z).\end{aligned}\tag{11}$$

All coefficients in these equations do not depend on x. The boundary conditions which are

$$\begin{aligned}X_0(\varepsilon, x, 0) &= 1\\ X_h(\varepsilon, x, l_0) &= 0\end{aligned}\tag{11'}$$

also do not depend on x. The required solutions are therefore functions $X_{0,h}(\varepsilon, z)$ of one position variable z instead of two (x, z). Equations (11) can therefore be simplified as:

$$\begin{aligned}&\Lambda\sin\theta_B\,\mathrm{d}X_0/\mathrm{d}z = i\exp\{i\varphi(z)\}X_h(\varepsilon, z)\\ &\quad - i\varepsilon h\Lambda\cos\theta_B X_h - \Lambda\sin\theta_B\,\mathrm{d}X_h/\mathrm{d}z\\ &\quad= i\exp\{-i\varphi(z)\}X_0(\varepsilon, z).\end{aligned}\tag{12}$$

As the coefficient $(\Lambda\sin\theta_B)$ does not depend on θ_B, the plane-wave reflectivity $\rho(\varepsilon) = |X_h(\varepsilon, 0)|^2$ depends on ε (and on θ_B) through the coefficient $\varepsilon\Lambda h\cos\theta_B$ only. Therefore, the integrated reflectivity obtained

by integration of $\rho(\varepsilon)$ over ε is proportional to $(\Lambda h \cos\theta_B)^{-1}$ and consequently to $\tan\theta_B$.

2.2. *Experiments*

The experiments were carried out on the S20 diffractometer at ILL, using a Ge(111) crystal as monochromator. The investigated crystal was an SiO_2 plate ($30\times30\times5$ mm) with the normal direction along [110]. The neutron diffraction properties of this crystal have been studied previously by Chalupa, Michalec & Galociova (1969) for a single wavelength (1·54 Å). The whole crystal surface was illuminated by the neutron beam, as illustrated in Fig. 2(*a*). The frequency of the thickness vibrations was 506 kHz.

It is simpler to measure for each wavelength the ratio of the intensities diffracted by the vibrating and the non-vibrating crystals, instead of measuring the absolute reflectivities (this would require a measurement of the incident-beam intensity). This ratio R is a function of the vibration amplitude (Fig. 3*a*), which is proportional to the intensity i of the current flowing through the crystal. No diminution of the increasing rate of R was observed in the available range of i, indicating that our measurements are far from the saturation regime (kinematical limit) which would be obtained with very large values of the vibration amplitude.

From the theoretical analysis of the preceeding section, R is expected to be independent of λ. This is in very good agreement, within the limits of the experimental errors, with the results shown in Fig. 3(*b*).

Diffraction topographs were used to check the homogeneity of the crystal reflectivity. For ideal

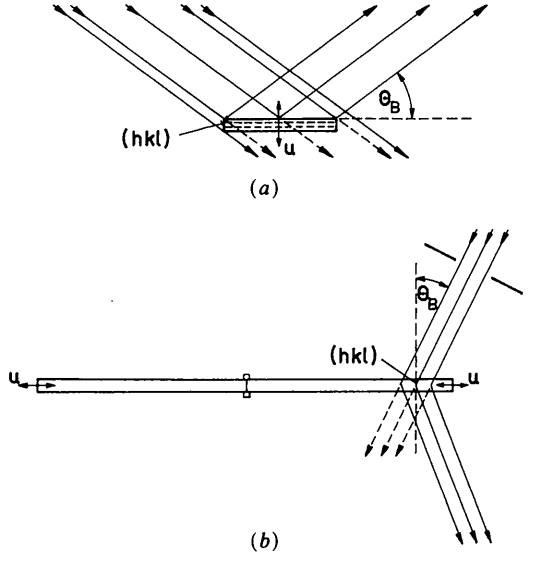

Fig. 2. Schematic arrangement for neutron diffraction by a vibrating single crystal: (*a*) thickness vibration mode; (*b*) longitudinal vibration mode.

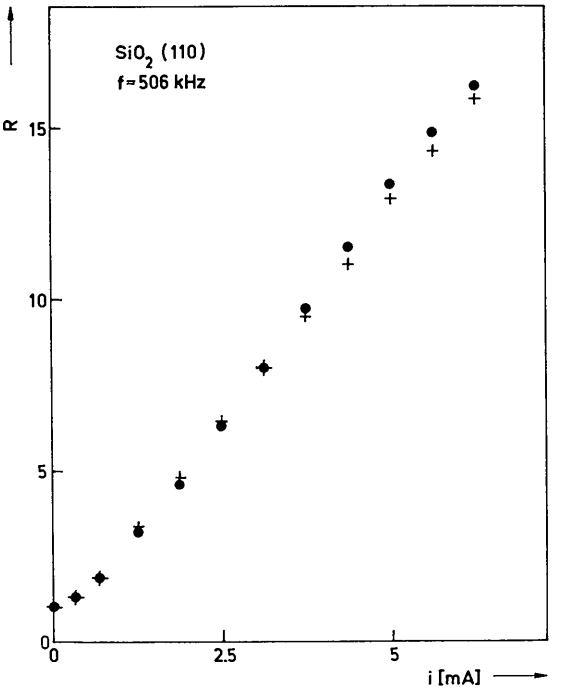

(*a*)

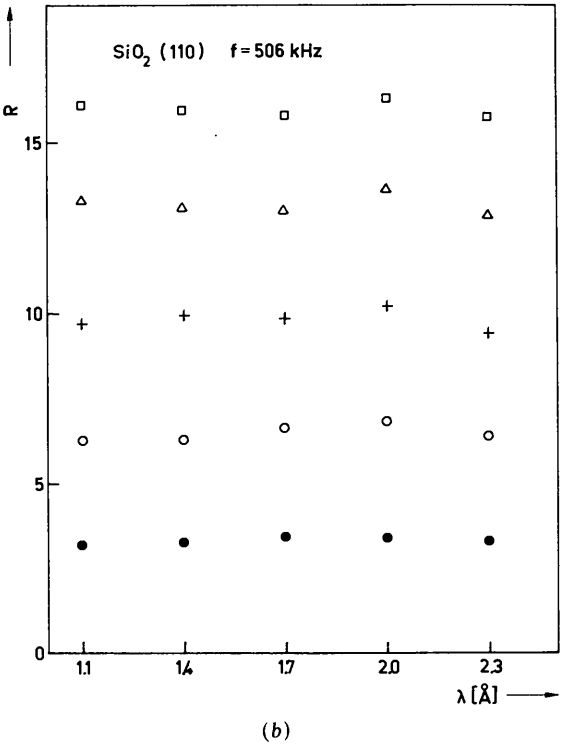

(*b*)

Fig. 3. (*a*) The dependence of the ratio R of the integrated reflectivities of a thickness mode of vibrating and non-vibrating quartz crystals on the effective value of the exciting high-frequency current i flowing through the crystal for the neutron wavelengths $\lambda = 1{\cdot}1$ Å (●) and $\lambda = 2{\cdot}3$ Å (+) (symmetrical Bragg reflection geometry). (*b*) *R versus* the neutron wavelength λ for different values of the high-frequency current i: ● 1·25 mA, ○ 2·5 mA, + 3·75 mA, △ 5·0 mA and □ 6·25 mA.

conditions, we should expect topographs of uniform intensity. This was not the case, but the experiments are, however, in good agreement with predictions based on these ideal conditions. This means that our theoretical analysis can be applied separately to different parts of the crystal in which the crystal deformation can be assumed to be homogeneous.

3. The symmetrical Laue case

3.1. *Theoretical background*

Consider the time-dependent displacement field $u(x, t)$ of resonant longitudinal vibrations along the x direction in a crystal bar, as illustrated in Fig. 2(b):

$$u(x, t) = u_0 \sin(\pi x/L) \sin(\omega t), \tag{13}$$

where L is the length of the bar and ω the circular frequency depending on the sound velocity c_x in the crystal ($\omega = \pi c_x/L$).

The scattering vector is parallel to the x direction, with displacement gradient u'_x, and the movement of the reflecting planes with velocity u'_t results in an x- and t-dependent shift of the interplanar spacing d [$d \to d + \Delta d(x, t)$]. In terms of the first derivatives of $u(x, t)$,

$$\Delta d(x, t) = d\{u'_x + u'_t/v \sin\theta_B\}, \tag{14}$$

where v is the neutron velocity. The second term in (14) represents the Doppler and aberration effects. Since v is inversely proportional to λ, $v \sin\theta_B$ does not depend on λ. Using the relation $\lambda = 2d \sin\theta_B$, we get the following x- and t-dependent shift $\Delta\theta(x, t)$ of the Bragg angle

$$\Delta\theta_B(x, t) = -\tan\theta_B\{u'_x + u'_t/v \sin\theta_B\}. \tag{15}$$

The lateral displacement δx and the time of flight δt along a neutron path in the crystal are proportional to $\tan\theta_B$ and are assumed to be much smaller than L and $t = 2\pi/\omega$ respectively:

$$\delta x = l_0 \tan\theta_B \ll L$$
$$\delta t = \frac{l_0}{v\cos\theta_B} = \frac{l_0}{v\sin\theta_B}\tan\theta_B \ll T. \tag{16}$$

Therefore the corresponding variation $\delta(\Delta\theta_B)$,

$$\delta(\Delta\theta_B) = [\partial(\Delta\theta_B)/\partial x]\delta x + [\partial(\Delta\theta_B)/\partial t]\delta t,$$

can be expressed in terms of second derivatives of $u(x, t)$:

$$\delta(\Delta\theta_B) = -(\tan\theta_B)^2 l_0\{u''_{xx} + (2/v\sin\theta_B)u''_{xt} + (1/v\sin\theta_B)^2 u''_{tt}\} \tag{17}$$

and is thus proportional to $(\tan\theta_B)^2$.

Kulda (1984) has shown that the integrated reflectivity of deformed crystals can be expressed as the product of the angular width $|\delta(\Delta\theta_B)|$ by the probability of being reflected for a neutron fulfilling the Bragg condition somewhere along its trajectory in the crystal. He has found

$$\rho = |\delta(\Delta\theta_B)|\{1 - \exp[-\rho_K/|\delta(\Delta\theta_B)|]\} \tag{18}$$

in which ρ_K is the kinematical limit. This is an approximation which supposes that $|\delta(\Delta\theta_B)|$ largely exceeds the Darwin width corresponding to a perfect crystal and that the Bragg condition can be fulfilled only once along any trajectory [otherwise, secondary extinction effects, as discussed by Mikula, Michalec, Chalupa, Sedláková & Petržilka (1975) should occur]. This last condition is satisfied in the case of our vibrating crystal because of conditions (16). The x- and t-dependent reflectivity $\rho(x, t)$ of the vibrating crystal is thus expected to be proportional to $(\tan\theta_B)^2$ if the vibration amplitude is not very small. This result is also valid for the integrated reflectivity which is obtained by integrating $\rho(x, t)$ over x and t and which is to be compared to the measurements.

3.2. *Experiments*

In these Laue-case experiments we have used longitudinal vibrations (Fig. 2) which have much larger amplitudes u_0 than the thickness vibrations used in the Bragg-case experiments, and it was possible to indicate the values of u_0 obtained by microscope observations instead of the intensity of the alternative current flowing through the crystal or through the piezoceramic transducer.

Our results for a perfect silicon crystal are shown in Figs. 4(a) and (b). The steady increase of the intensity ratio R as a function of the vibration amplitude u_0 shows that we are far from the kinematical limit in the whole available u_0 range. Since the perfect-crystal reflectivity is proportional to $\tan\theta_B$, the ratio $R/\tan\theta_B$ should be independent of λ if the vibrating-crystal reflectivity is proportional to $(\tan\theta_B)^2$. It is shown in Fig. 4(b) that the relative changes of the measured values of $R/\tan\theta_B$ are indeed very small except for the lowest considered value of u_0.

Similar results for a crystal of quartz which is known to be less perfect than the crystal of silicon but enabled us to use much larger vibration amplitudes are displayed in Figs. 5(a) and (b). Inspection of Figs. 4(a) and 5(a) reveals that the tendency of the intensity *vs* u_0 to reach saturation [as predicted by (18)] is more visible in the case of the quartz crystal. In fact, the saturation would be fully achieved only by using extremely large vibration amplitudes, which could not be experimentally realized in our studies. For our treatment we have chosen a minimum value u_0^* in the linear range of the intensity dependence and in Fig. 5(b) we have considered the ratio $\rho_v(u_0)/\rho_v(u_0^*)$ for u_0 larger than u_0^*. The results show that this ratio does not depend on λ, even for vibration amplitudes large enough that the tendency to saturation starts to be present. This suggests that the

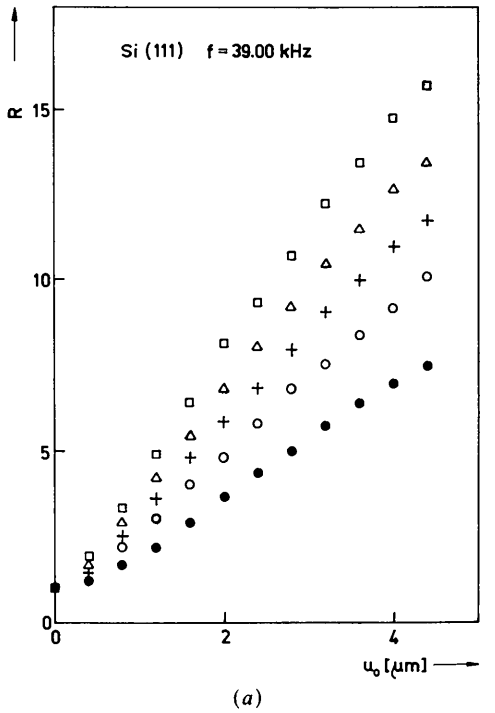

(a)

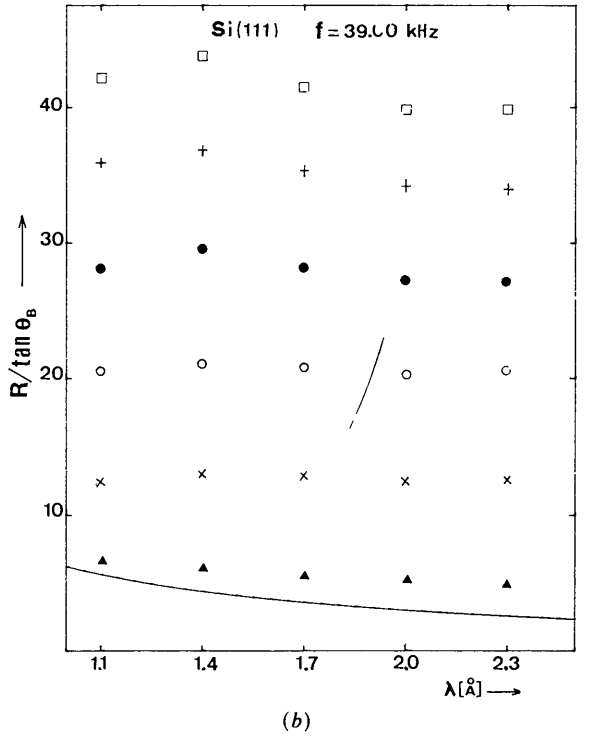

(b)

Fig. 4. (*a*) *R versus* the vibration amplitude u_0 of a longitudinally vibrating silicon bar for different values of λ: ● 1·1 Å, ○ 1·4 Å, + 1·7 Å, △ 2·0 Å and □ 2·3 Å (symmetrical Laue transmission geometry). (*b*) $R/\tan\theta_B$ *versus* neutron wavelength. R is the ratio of the reflectivities of the vibrating and non-vibrating crystals. The full curve represents the variations of $1/\tan\theta_B$. These results show the relative changes of $R/\tan\theta_B$ as a function of λ. Vibration amplitude u_0: □ 4·4 μm, + 3·6 μm, ● 2·8 μm, ○ 2 μm, × 1·2 μm, ▲ 0·4 μm (symmetric Bragg geometry).

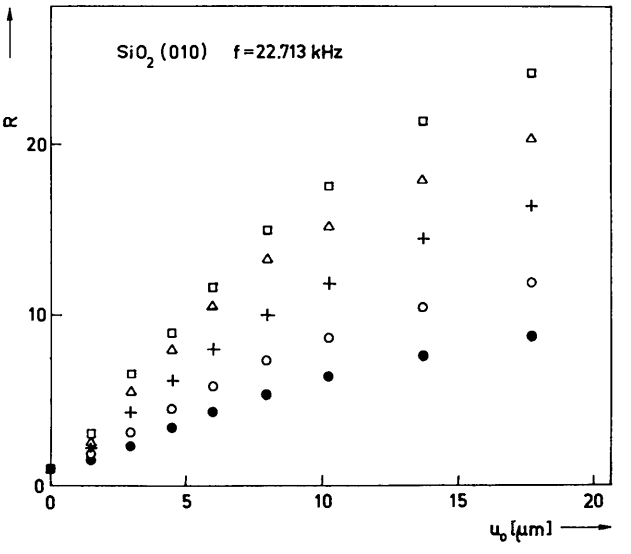

(a)

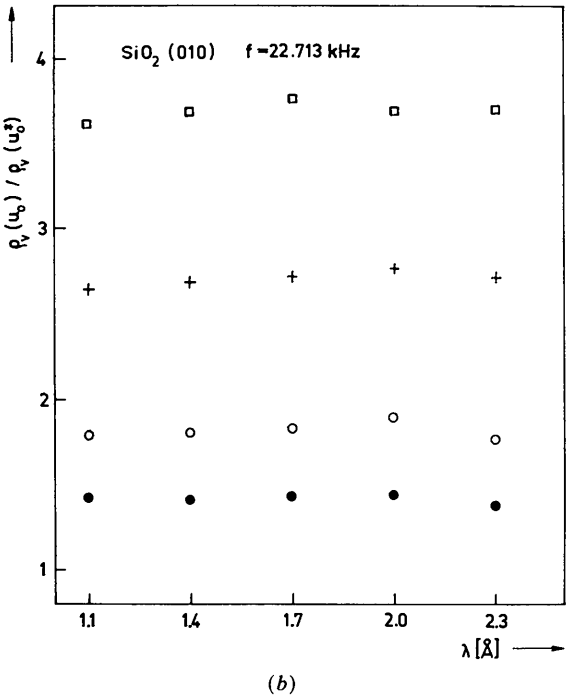

(b)

Fig. 5. (*a*) *R vs* the vibration amplitude u_0 of a longitudinally vibrating quartz bar for different values of λ: ● 1·1 Å, ○ 1·4 Å, + 1·7 Å, △ 2·0 Å and □ 2·3 Å (symmetric Laue transmission geometry). (*b*) The ratio of the integrated reflectivities of the longitudinally vibrating quartz crystal $\rho_v(u_0)$ with respect to $\rho_v(u_0^*)$ *vs* λ for different values of u_0: ● 4·5 μm, ○ 6 μm, + 10 μm, □ 17·5 μm and $u_0^* = 3$ μm.

$(\tan \theta_B)^2$ dependence of the reflectivity which holds for the kinematical limit is also satisfied in the range of the vibration amplitudes above the value u_0^*. This is in agreement with our theoretical prediction based on (18).

4. Concluding remarks

We have investigated the dependence on the neutron wavelength of the integrated reflectivity of perfect and nearly perfect vibrating crystals in symmetrical diffraction geometries, the vibration vector **u** being always parallel to the diffraction vector **h**. We have verified the predictions of the wave-optical theory developed for the Bragg case and which is valid for any value of the vibration amplitude, from the perfect crystal to the kinematical limit. In the Laue case, our measurements could be used to discuss the rather large range of validity of (18) which is a simple approximation for the reflectivity of a deformed crystal.

The authors are grateful to Dr R. Michalec for kindly lending the quartz crystals and to Mr A. Dvorak for his help with the preparation of the manuscript.

References

CHALUPA, B., MICHALEC, R. & GALOCIOVA, D. (1969). *Nucl. Instrum. Methods*, **67**, 357-358.
GUIGAY, J. P. (1986). *Acta Cryst.* A**42**, 481-483.
KULDA, J. (1984). *Acta Cryst.* A**40**, 120-126.
KULDA, J. & LUKÁŠ, P. (1989). *Phys. Status Solidi B*, **153**, 435-442.
KULDA, J., VRÁNA, M. & MIKULA, P. (1988). *Physica (Utrecht)*, B**151**, 122-129.
MICHALEC, R., CHALUPA, B., SEDLÁKOVÁ, L., MIKULA, P., PETRŽILKA, V. & ZELENKA, J. (1974). *J. Appl. Cryst.* **7**, 588-592.
MICHALEC, R., MIKULA, P., VRÁNA, M., KULDA, J., CHALUPA, B. & SEDLÁKOVÁ, L. (1988), *Physica (Utrecht)*, B**151**, 113-121.
MIKULA, P., MICHALEC, R., CHALUPA, B., SEDLÁKOVÁ, L. & PETRŽILKA, V. (1975). *Acta Cryst.* A**31**, 688-693.
TAKAGI, S. (1962). *Acta Cryst.* **15**, 1311-1312.
TAKAGI, S. (1969). *J. Phys. Soc. Jpn*, **26**, 1239-1253.
TAUPIN, D. (1964). *Bull. Soc. Fr. Minéral. Cristallogr.* **87**, 469-511.

Acta Cryst. (1990). A**46**, 826-831

Euklidische Normalisatoren für trikline und monokline Raumgruppen bei spezieller Metrik des Translationengitters

VON ELKE KOCH

Institut für Mineralogie der Universität Marburg, Hans-Meerwein-Strasse, D-3550 Marburg, Deutschland

UND ULRICH MÜLLER

Fachbereich Chemie der Universität Marburg, Hans-Meerwein-Strasse, D-3550 Marburg, Deutschland

(*eingegangen am* 2 *April* 1990; *angenommen am* 20 *Juni* 1990)

Abstract

A listing of the Euclidean normalizers for triclinic and monoclinic space groups having translation lattices with specialized metric is given. These normalizers have not been included in previous tabulations. For convenience, in the case of monoclinic space groups, only the second setting (*c*-axis unique) is considered and the metric of the cells is restricted within certain limits which warrant that all specialized cases and all cell choices according to *International Tables for Crystallography* [(1987) Dordrecht: Kluwer] are included.

Die zunehmende Bedeutung des Konzepts der euklidischen und affinen Normalisatoren von Raumgruppen wird auch durch die Aufnahme entsprechender Tabellen in die neueste Auflage des Bandes A der *International Tables for Crystallography* verdeutlicht (Koch & Fischer, 1987). Ebenso wie in früheren Zusammenstellungen (Hirshfeld, 1968; Gubler, 1982*a*, *b*; Fischer & Koch, 1983) sind dort die euklidischen Normalisatoren aber nur für solche Raumgruppen aufgeführt, deren Translationengitter keine speziellen metrischen Eigenschaften haben. Entspricht bei einem bestimmten Raumgruppenexemplar die Gittermetrik aber einer höheren Kristallfamilie, d.h. gehört die Punktgruppe des Gitters zu einer anderen Familie als die Raumgruppe selbst, dann kann der zugehörige euklidische Normalisator ebenfalls eine höhere Symmetrie haben als es dem Normalfall für diesen Raumgruppentyp entspricht.

Der euklidische Normalisator einer jeden Raumgruppe ist eine Untergruppe ihres affinen Normalisators. Beide Normalisatoren sind für den allgemeinen Fall, d.h. bei nicht spezialisierter Metrik

0108-7673/90/100826-06$03.00